

DISSIPATION TEST EVALUATION WITH A POINT-SYMMETRICAL CONSOLIDATION MODEL

Emőke IMRE and Pál RÓZSA

Geotechnical Research Group of the Hungarian Academy of Sciences at the Department of
Geotechnics,

Department of Computer Science and Information Theory
Budapest University of Technology and Economics
H–1521 Budapest, Hungary

Received: Dec. 14, 2005

Abstract

A point-symmetrical linear coupled consolidation model with constant displacement boundary condition is tested against measured dissipation test data. Results show that – similarly to the previously tested cylindrical model – very short data jets can successfully be evaluated if the sensor is well above the tip.

Keywords: dissipation test, inverse problem, analytical solution, coupled consolidation model.

1. Introduction

The dissipation test evaluation needs a model (including an initial condition); an inverse problem solver (including the reliability testing of the inverse problem solution) and, some measured data.

Presently either 2D model with numerical solution or 1D models with analytical solution are used. The initial condition is produced either with the strain path method or with the cavity expansion method or simply identified during model fitting [11][12][3][7, 8].

The non-linear inverse problem solution is generally approximate. The approximate dissipation test evaluation methods can be divided into three groups:

- i one point fitting methods (e.g. using the 50 % dissipation time t_{50}),
- ii slope type fitting methods using the slope of the first straight line portion of the u versus $t^{0.5}$ plot,
- iii trial and error procedure, the reliability of the identified parameters is not tested [12].

In the dissipation testing the measurement is made using various filter positions (*Fig. 1*). The shaft positions are mostly used for research purpose, the cone-close positions A, B, C (*Fig. 1c*) or u_1 , u_2 , (*Fig. 1d*) are applied in practice. The testing time (e.g. 50 % dissipation time t_{50} , (see *Table 1*) is relatively long.

In this paper a new evaluation method is presented. The model is analytical, a spherical coupled consolidation model [6]. The shape of the initial condition is

identified, the size of the displacement domain is determined with the strain path method.

The non-linear inverse problem is solved precisely, in an automatic way entailing some reliability testing as well [4].

In this paper this method is tested against measured dissipation test data related to five filter positions A to E (Figs. 1c, 2). According to the results, the method is powerful if the sensor is well above the tip (shaft position). In this case the necessary testing time is about 2 minutes only.

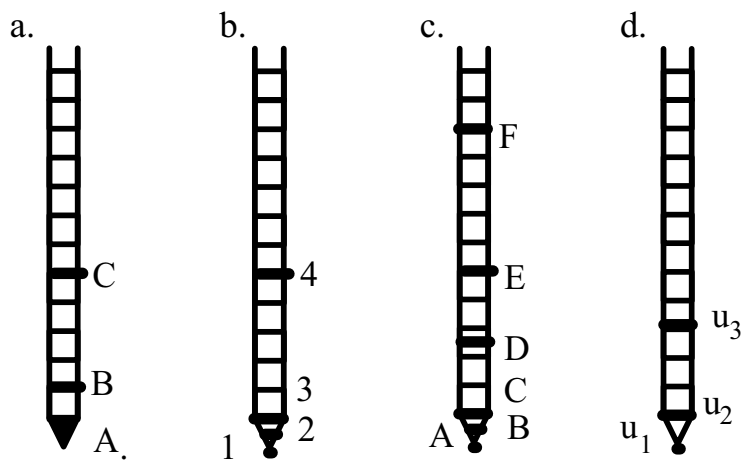


Fig. 1. Some filter positions known from the literature. a. [15], b. [2], c. [14], d. [9]

2. Model, Model Law

The system of differential equations of the 3-dimensional coupled linear point-symmetrical consolidation model:

$$E_{oed} \frac{\partial}{\partial r} \frac{1}{r} \frac{\partial}{\partial r} (rv) - \frac{\partial u}{\partial r} = 0 \quad (1)$$

$$-\frac{k}{\gamma_v} \frac{1}{r} \frac{\partial}{\partial r} \left(r \frac{\partial u}{\partial r} \right) + \frac{\partial}{\partial t} \frac{1}{r} \frac{\partial}{\partial r} (rv) = 0 \quad (2)$$

where u [kPa] is pore water pressure, v [m] is displacement, r [m] is the space co-ordinate and, t [s] is time, k [m/s] is permeability, γ_v [kN/m³] is unit weight of water, E_{oed} [kPa] is oedometric modulus.

The boundary conditions are as follows:

$$u(t, r) |_{r=r_1} = 0 \quad (3)$$

$$\frac{\partial u(t, r)}{\partial y} |_{r=r_0} \equiv 0 \quad (4)$$

$$v(t, r) |_{r=r_0} \equiv v_0 > 0 \quad (5)$$

$$v(t, y) |_{r_1} \equiv 0 \quad (6)$$

In this work the distance $r = r_0$ was the radius of the rod, r_1 was taken as the distance being perpendicular to the approximate zero excess pore water pressure line given by the strain path method [1], depending on the filter position. The so determined value of r_1 was $22r_0$, $23r_0$, $24r_0$, $31r_0$ for A, B, C, D respectively, Fig. 3.

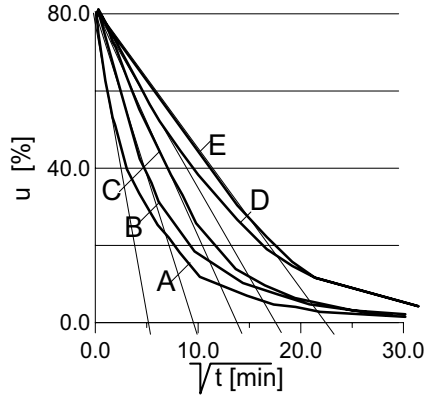


Fig. 2. Data of Lunne et al (1992) in u versus $t^{0.5}$ plot (filter positions are shown in (Fig. 1c))

The analytical solutions for u and for the transient part of the displacement v^t are as follows:

$$u(t, r) = 1/\sqrt{r} \sum_{k=1}^{\infty} \lambda_k C_k e^{-\gamma_k^2 \cdot c \cdot t} \left\{ \begin{array}{l} [J_{0.5}(\lambda_k r) + \mu_k Y_{0.5}(\lambda_k r)] \\ -[J_{0.5}(\lambda_k r_1) + \mu_k Y_{0.5}(\lambda_k r_1)] \end{array} \right\} \quad (7)$$

$$v^t(t, r) = 1/\sqrt{r} \sum_{k=0}^{\infty} C_k e^{-\lambda_k^2 \cdot c \cdot t} [J_{1.5}(\lambda_k r) + \mu_k Y_{1.5}(\lambda_k r)] \quad (8)$$

where c [m^2/s] is coefficient of consolidation:

$$c = \frac{k \cdot E_{oed}}{\gamma_v} \quad (9)$$

J_r/Υ_r are Bessel functions of the first and second kinds, with the order of r . The coefficients C_k ($k = 1 \dots \infty$) [kPa] are to be determined from the initial transient

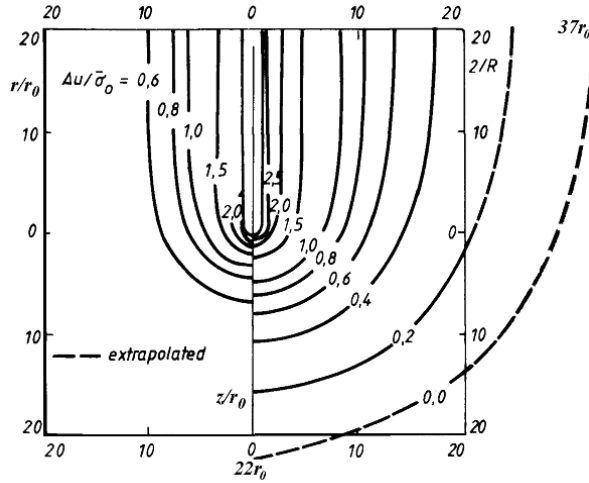


Fig. 3. Pore pressure results of the strain path method (undrained penetration, after [1]). Left and right: bilinear and hyperbolic modelling. Distances/excess pore water pressure are normalized by pile radius/initial effective isotropic stress, respectively.

displacement function $v_0'(r)$ (in this work it is identified from measured data). The parameters λ_k [1/m] and μ_k [-] ($k=1\dots\infty$) are the roots of the boundary condition equations (8) and (9) what can be compiled as follows:

$$J_{1.5}(\lambda_k r_1)/J_{1.5}(\lambda_k r_0) = Y_{1.5}(\lambda_k r_1)/Y_{1.5}(\lambda_k r_0) \quad (10)$$

This equation can be modified by using the asymptotic formulae:

$$J_{1.5}(r) = \sqrt{2/r\pi} \cos(r - \pi/4 - 3\pi/4) \quad (11)$$

$$Y_{1.5}(r) = \sqrt{2/r\pi} \sin(\pi/4 - 3\pi/4) \quad (12)$$

resulting in the following approximate boundary condition equation and roots:

$$\sin(\lambda_k(r_1 - r_0)) = 0 \quad (13)$$

$$\lambda_k = \frac{k\pi}{(r_1 - r_0)} \quad (14)$$

Inserting this into the analytical solution the resulting approximate solutions contain two dimensionless arguments $T=ct/(r_1 - r_0)^2$ time factor and, $R=r/(r_1 - r_0)$.

An important consequence of the existence of the approximate time factor T :

$$T = \frac{ct}{(r_1 - r_0)^2}$$

If T and t are specified, then an approximate relation does exist among the values of c and r_1 :

$$\frac{c_1}{(r_{1,1} - r_0)^2} \approx \frac{c_2}{(r_{1,2} - r_0)^2} \quad (15)$$

3. Inverse Problem Solution

3.1. Minimization

The merit function was defined as follows:

$$F(p) = \frac{\sqrt{\sum_{i=1}^N u_m(t_i) - u(t_i, p)}}{N_{\max}(u_m(t_i))} \quad (16)$$

where N is number of data, m measured, p is parameter vector consisting of c and C_k , ($k=1..20$). Results are presented for $k=1$.

The merit function was geometrically explored by applying a sub-minimization [4]. The global minimum was precisely determined.

3.2. Reliability Testing

The global minimizer p is reliable if it is the unique solution of the inverse problem and, if the confidence interval is within the range of p .

The error can analytically be estimated by computing the 88% confidence interval from the Tschebiseff inequality:

$$P(|x_i - p_i| \geq a) \leq \frac{\sigma_i^2}{a^2}, a > 0 \quad (17)$$

where x_i and σ_i are expected (identified) value and standard deviation of the parameter p_i , respectively.

The reliability criteria can be formulated in a geometrical way as well. The solution is unique if the merit function has a nice single global minimum point. The parameter error is acceptable if the merit function is not too flat around the global minimum point in agreement with the geometrical meaning of the standard deviation [13]. The deeper the valley, less is the standard deviation (Fig. 4).

The uniqueness and the parameter error were visualized by the construction of the so called minimal section of the merit functions with respect to c (Fig. 4, [4]). These are the flattest possible sections with respect to parameter c .

For very short data series, the standard deviation was not computed due to the very few data.

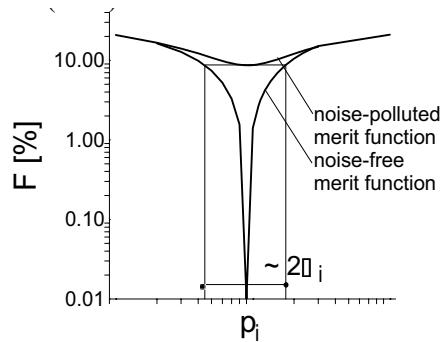


Fig. 4. Geometrical concept of the standard deviation of parameter p_i using the lower boundary of the orthogonal projection of the merit function onto the plane $F - p_i$ (called as minimal section concerning parameter p_i , [4]).

Instead of this simply the ‘width’ of the valley of the minimal sections of the noise-free merit function was inspected.

4. Results

For the parameter identification $r_1 = 37r_0$ (good for filter position E) was used then the identified c was modified using the model law (10) and the real values of r_1

For the parameter identification different test durations (t , the same notation is used as for the time variable) were used to test the relation between the identified c and the testing time.

According to the results (Tables 1-2, Figs. 5-8), the length of the data jet t practically did not influence the identified c for filter position E, and influenced in an increasing extent the identified c for filter positions A to D.

When c was modified according to the real value of r_1 , then it became about the same for every filter position if the test was long ‘enough’ (Table 2).

For long data jets, the fit was the best in filter position E and the worst in A. The variance (σ_c/c) increased between filter positions E to A and, the lower boundary of the 88% confidence interval ($c-3\sigma_c$) was negative except for filter positions C and E. Accordingly, the vicinity of the global minimum of the merit function for filter position E was nicer than for filter position A (Fig. 7).

For short data sets, filter position E, the shape of the minimal section of the merit function was practically unchanged with decreasing testing time t indicating that the solution is reliable (Fig. 8).

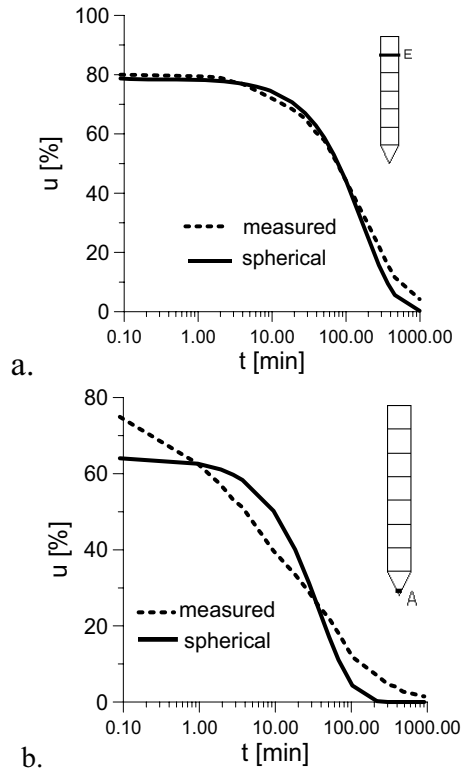


Fig. 5. Measured versus fitted data, filter position E (a) and A (b), point-symmetrical model.

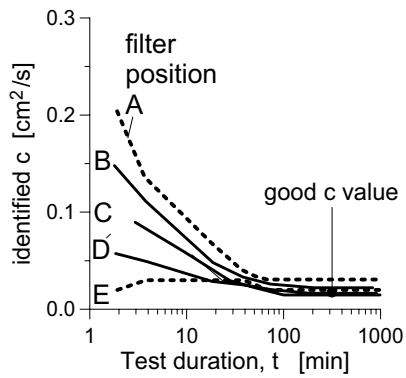


Fig. 6. Identified c with test duration t , spherical model

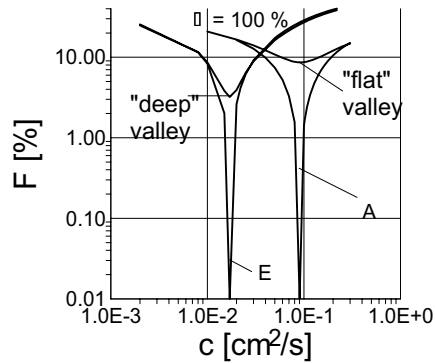


Fig. 7. The minimal section of the merit function with respect to the unmodified c (point-symmetrical model, long tests)

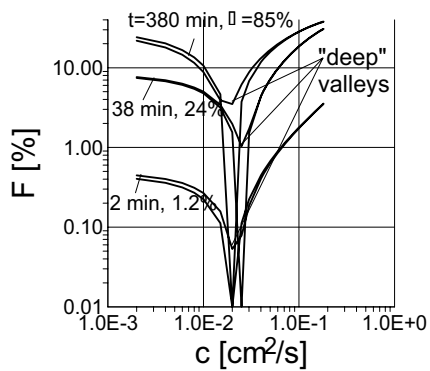


Fig. 8. The minimal section of the merit function with respect to c (point-symmetrical model, short tests, filter position E).

5. Discussion

5.1. Results of Approximate Identification Methods

Value of measured t_{50} varies from 22 to 100 min (Table 3). Using this and 150 for the rigidity index the one point fitting with t_{50} provides a c value of $0.15 \text{ cm}^2/\text{s}$ for both filter positions B and C.

The slope type approximate method results in values of c of $0.15 \text{ cm}^2/\text{s}$ and, of $0.015 \text{ cm}^2/\text{s}$ for filter positions B and C, respectively. The slope can be determined from an at least 5 min long part of the test (Fig. 2).

Table 1. The identified and modified coefficient of consolidation (c) and, the fitting error (F , σ_c/c) for long data sets

Filter position	Fitting error		c [cm ² /s]	
	F [%]	Coefficient of variation σ_c/c [-]	identified ($r_1=64.75$ cm)	modified with the model law and real value of r_1
A	9	0.57	0.09	0.0318
B	8	0.47	0.06	0.023
C	5	0.28	0.04	0.018
D	6	0.35	0.02	0.015
E	4	0.21	0.02	0.02

Table 2. The identified c [cm²/s] modified with the model law, short data jets, spherical model

Test duration t [min]	Filter position				
	A	B	C	D	E
~ 2	0.20	0.15	0.06	0.09	0.02
~ 4	0.10	0.11	0.05	0.06	0.03
~ 18	0.04	0.05	0.03	0.03	0.03
~ 37	0.03	0.03	0.02	0.02	0.03
~ 68	0.02	0.03	0.02	0.02	0.02
~ 217	0.03	0.02	0.02	0.02	0.02

The ‘true’ value of c is 0.01 cm²/s [10], or 0.0095 cm²/s [3].

Table 3. Approximate 50 % dissipation time t_{50} and 90 % dissipation time t_{90} (on the basis of [12])

Filter position	t_{50} [min]	t_{90} [min]
A	8	200
B	22	250
C	60	300
D	90	>600
E	110	>600

5.2. Results of Cylindrical Model

Some results of the previously tested cylindrical model [5, 7, 8] are shown in *Fig. 9* and in *Table 4*). Results show that the point-symmetrical model is slightly better than the previously tested cylindrical model.

In filter position E both models give good estimation for c ($0.02 \text{ cm}^2/\text{s}$) even from a 2 min long test.

In filter positions A to D the fitting error is greater and c is dependent on the testing time (*Figs 6, 9*). If c is identified from a test being longer than 20-40 min then c is acceptable (*Table 4*).

Table 4. The identified and modified coefficient of consolidation (c) and, the fitting error for long data sets

Filter position	Fitting error		c [cm^2/s]	
	F [%]	Coefficient of variation σ_c/c [-]	identified assuming $r_1=64.75\text{cm}$	modified with the model law and real value of r_1
A	9	0.56	0.13	0.045
B	8	0.45	0.09	0.0345
C	5	0.28	0.06	0.027
D	6	0.37	0.03	0.0225
E	4	0.23	0.02	0.02

5.3. Test Duration

According to the results (*Tables 1-4, Figs. 5-9*), the identified c was independent of the testing time t for filter position E, and was dependent on the the testing time t for filter positions A to D.

These results imply that the consolidation is one dimensional about 5 diameter above the shoulder and the two dimensional nature can not be neglected below this level. This implication is comparable with the results of 2D consolidation analyses where the 1D nature of the dissipation is acceptable around the shaft from about 2.5 D above the shoulder (e.g.*Fig.10*, [14]).

It can also be mentioned that presently both the shaft element and the pore water elements (A, B, C in *Fig. 1c* or u_1, u_2 in *Fig. 1d*) are situated in some cone-close positions which is probably not the optimal place from the point of view of the evaluation being the consolidation 2D here. (Generally the measured local side friction data are not used for pile capacity design probably because of this reason.)

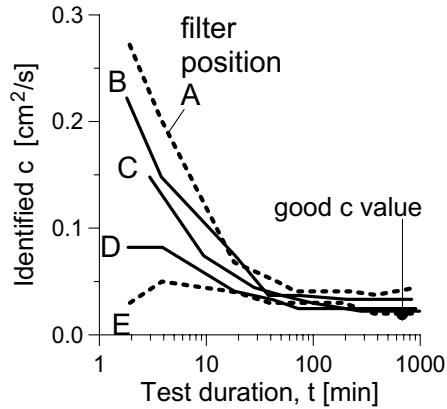


Fig. 9. Identified c with test duration t , cylindrical model.

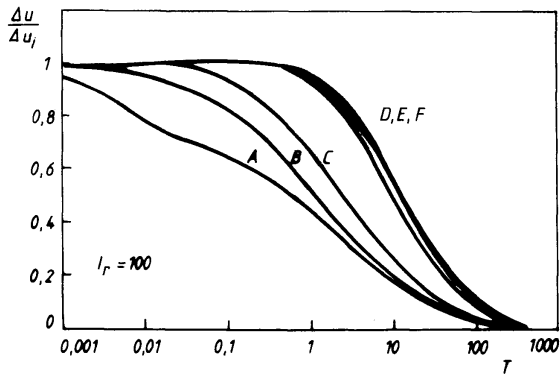


Fig. 10. Simulated dissipation test results (after [14])

6. Conclusion

The suggested evaluation procedure versus approximate methods

The suggested evaluation procedure differs from the widely used methods as follows:

- i the model is 1D coupled and analytical (generally 2D uncoupled numerical solutions are used),
- ii the non-linear inverse problem solution method is precise and automatic (generally approximate solutions are adopted),
- iii the initial condition is identified (generally separate theory is used which needs additional parameters),

iv the reliability of the inverse problem solution is tested.

The approximate evaluation methods generally over-predict the value of c by about one order of magnitude using sampling times of about 5 min to 100 min. No information is given for the reliability of the solution of the inverse problem.

The suggested automatic evaluation methods give good value for c for shaft filter position E using sampling time of 2 min only (less than the time needed for the approximate methods).

For other filter positions the necessary testing time is about 20-40 min (comparable with the approximate methods presently used, but the result is more precise).

An inference of the results

The presently used shaft elements are situated immediately above the shoulder at present.

In the dissipation testing the measurements are generally made using some cone-close positions (A, B, C in *Fig. 1c* or u_1, u_2, u_3 in *Fig. 1d*).

Table 5. Cylindrical model, the coefficient of consolidation c [cm^2/s] from short data jets

Test duration t [min]	Filter position				
	A	B	C	D	E
~ 2	0.27	0.22	0.08	0.14	0.02
~ 4	0.20	0.15	0.08	0.07	0.03
~ 18	0.07	0.07	0.04	0.04	0.03
~ 37	0.05	0.04	0.03	0.03	0.03
~ 68	0.04	0.04	0.02	0.03	0.02
~ 217	0.04	0.03	0.02	0.02	0.02

The results presented here imply that the consolidation is one dimensional about 5 diameter above the shoulder and the two dimensional nature can not be neglected below this level.

On the basis of the results of this research it can be suggested that the position of both the shaft elements and the filters is advisable to be moved well above the tip (5 diameter above the shoulder is suggested).

References

- [1] BALIGH, M. M., Undrained Deep Penetration, II. Pore Pressures *Geotechnique*, **36(4)** (1986) pp. 487–503.
- [2] BALIGH, M. M. – LEVADOUX, J. N., Consolidation after Undrained Penetration. II. Interpretation. *Jl. of Geot. Eng. ASCE*, **112** (1986) (6), pp. 727–747.

- [3] BURNS, S.E., MAYNE, P.W (1995). Coefficient of Consolidation (c_h) from Type 2 Piezocone Dissipation Test in Overconsolidated Clay, *Proc. of Int.Symp. on CPT*. pp. 137–142.
- [4] IMRE, E. (1996). Inverse Problem Solution with a Geometrical Method. *Proc. of the 2nd Int. Conf. on Inverse Problems in Engineering*, Le Croisic, France. pp. 331–338.
- [5] IMRE, E. – RÓZSA, P., Consolidation around Piles, *Proc. of 3rd Seminar on Deep Foundations on Bored and Auger Piles. Ghent (1998)*, pp. 385–391.
- [6] IMRE, E. – RÓZSA, P., Modelling for Consolidation around the Pile Tip, *Proc. of the 9th Int. Conf. on Piling and Deep Foundations (DFI), Nizza, 2002*, pp. 513–519.
- [7] IMRE, E., Evaluation of ‘Short’ Dissipation Tests, *Proc. of the 12th Danube-European Conference, (2002a)*, pp. 499–503.
- [8] IMRE, E.(2002b). Pile consolidation models and scale effect. *Proc. of NUMGE 2002. Paris*.
- [9] KIM, Y.S. – LEE, S. R. – KIM, Y. T., Application of an Optimum Design Technique for Determining the Coefficient of Consolidation by Using Piezocone Test Data. *Computers and Geotechnics* **21/4** (1997) pp. 277–293.
- [10] LEHANE, B. M. – JARDINE, R. J., (1994) Displacement-pile Behaviour in a Soft Marine Clay *Canadian Geotechnical Journal*. **31** pp. 181–191.
- [11] LEVADOUX, J. – BALIGH, M. M. (1986). Consolidation after Undrained Penetration I. Prediction. *Jl. of Geot. Eng. ASCE* 112(6): pp. 707–727.
- [12] LUNNE, T. – ROBERTSON, P. K. – POWELL, J. J. M. (1992). *Cone Penetration testing*. Blackie Academic & Professional.
- [13] PRESS, W. H. – FLANNERY, B. P. – TEUKOLSKY, S.A. – WETTERLING, W.T. (1986): *Numerical Recipes*. Cambridge Univ. Press.
- [14] TEH, C. I. – HOULSBY, G. T., Analysis of the Cone Penetration Test by the Strain Path Method, *Proc. 6th Int. Conf. on Num. Meth. in Geomechanics, Innsbruck (1988)*.
- [15] TORSTENSSON, B. A., *The Pore Pressure Probe*, (1977) Paper No. 34. NGI